NASA TECHNICAL MEMORANDUM

NASA TM X-3362

NASA TM X-3362

HEAT-TRANSFER CHARACTERISTICS OF PARTIALLY FILM COOLED PLUG NOZZLE ON A J-85 AFTERBURNING TURBOJET ENGINE

Stanley M. Nosek and David M. Straight

Lewis Research Center
Cleveland, Ohio 44135

NATIONAL AERONAUTICS AND SPACE ADMINISTRATION • WASHINGTON, D. C. • MARCH 1976

1. Report No.	2. Government Accession No.	3. Recipient's Catalog No.
NASA TM X-3362		

4. Title and Subtitle	5. Report Date
HEAT-TRANSFER CHARACTERISTICS OF PARTIALLY FILM COOLED PLUG NOZZLE ON A J-85 AFTERBURNING TURBOJET ENGINE	March 1976
	6. Performing Organization Code

7. Author(s)	8. Performing Organization Report No.
Stanley M. Nosek and David M. Straight	E-8553
	10. Work Unit No.
	505-04

9. Performing Organization Name and Address	11. Contract or Grant No.
Lewis Research Center National Aeronautics and Space Administration Cleveland, Ohio 44135	
	13. Type of Report and Period Covered
12. Sponsoring Agency Name and Address	Technical Memorandum
National Aeronautics and Space Administration Washington, D. C. 20546	14. Sponsoring Agency Code

15. Supplementary Notes

16. Abstract

Plug nozzle film-cooling data were obtained downstream of a slot located at 42 percent of the total plug length on a J-85 engine. Film cooling reduced the aft end wall temperature as much as 150 K (250^{0} R), reduced total pressure loss in the upstream convection cooling passages by 50 percent, and reduced estimated compressor bleed flow requirement by 14 percent compared to an all convectively cooled nozzle. Shock waves along the plug surface strongly influenced temperature distributions on both convection and film cooled portions. The effect was most severe at nozzle pressure ratios below 10 where adverse pressure gradients were most severe.

17. Key Words (Suggested by Author(s))	18. Distribution Statement
Turbine exhaust nozzles; Plug nozzles; Exhaust nozzles; Film cooling; Cooling; Supersonic heat transfer; Shock wave interaction; Heat transfer	Unclassified - unlimited STAR Category 07

19. Security Classif. (of this report)	20. Security Classif. (of this page)	21. No. of Pages	22. Price*
Unclassified	Unclassified	30	$3.75

* For sale by the National Technical Information Service, Springfield, Virginia 22161

HEAT-TRANSFER CHARACTERISTICS OF PARTIALLY FILM COOLED PLUG NOZZLE ON A J-85 AFTERBURNING TURBOJET ENGINE

by Stanley M. Nosek and David M. Straight

Lewis Research Center

SUMMARY

As part of a continuing investigation on plug nozzles, a partially film cooled plug nozzle was tested at exhaust gas temperatures up to 2040 K (3675° R). An annular film cooling slot was located 42 percent of the plug length downstream of the nozzle's primary throat. The plug surface upstream of the film cooling slot was convectively cooled. Data were obtained over a range of coolant flow rates and nozzle pressure ratios at several nozzle inlet pressures and temperatures.

A comparison of the film cooled plug with a convectively cooled plug which was truncated at 60 percent of its full length showed a 90 to 150 K (160° to 250° R) reduction in wall temperatures between the 42 and 60 percent plug locations for the film cooled configuration. In addition, the total pressure loss of the convectively cooled portion of the plug decreased about 50 percent and the plug coolant flow necessary to keep the plug surface below its design maximum of 1220 K (2200° R) was estimated to be reduced by 14 percent to 3.0 percent of compressor flow. (The all convectively cooled plug required 3.5 percent of compressor flow.)

The temperature distributions along the surface of the plug for both the convection and film cooled regions were strongly influenced by shock waves. Cooling the plug was most difficult at nozzle pressure ratios below 10 where shock waves produced the most severe adverse pressure gradients along the plug surface.

INTRODUCTION

An investigation was conducted with a J-85 afterburning turbojet engine to obtain heat transfer characteristics of a plug-type exhaust nozzle incorporating convection and partial film cooling. Past investigations of plug nozzle designs at the Lewis Research Center (refs. 1 to 8) have demonstrated their capability of improving thrust performance over that of other nozzle configurations for a wide range of engine operating conditions.

These previous tests, however, were conducted with uncooled plug nozzle designs. Because of the high operating temperatures of afterburning gas turbine engines, it becomes imperative to cool the surfaces exposed to the hot exhaust gases for any proposed plug nozzle design. In addition, for the plug nozzle to be given serious consideration, the design requires an efficient cooling scheme which minimizes cooling flow requirements, is relatively light in weight, and avoids complexity.

The methods that are commonly considered for cooling nozzles are convection, film cooling or a combination of both. These methods as applied to plug nozzles have been investigated at the Lewis Research Center (refs. 9 to 16). References 9, 10, and 11 present the experimental results with a convectively cooled plug nozzle installed on an afterburning J-85 turbojet engine. In the work described in references 9 and 10, the plug was truncated at the 60 percent location downstream of the nozzle throat. The coolant was discharged in a downstream direction at sonic velocity from an annular slot at the point of truncation to recover some thrust from the coolant stream. For the flight tests described in reference 11, the plug was convectively cooled to 60 percent of the length and the remaining 40 percent was film cooled. Although these investigations demonstrated the feasibility of the cooling designs used, the resulting nozzle system was complex and heavy.

The study described in reference 12 resulted in potential reductions in weight and cooling flow requirements of several partial film cooled plug nozzle configurations compared to an all convection cooled design. Some concern, however, has been expressed over the effect of shock and recompression waves along the plug surface on the film cooling effectiveness, particularly at the off-design conditions (ref. 10).

Experimental investigations in altitude facilities using small film cooled models (21.6-cm (8.5-in.) model diameter) are reported in references 13 to 16. References 13 and 14 present the thrust performance and heat transfer results of models tested at gas temperatures up to 555 K (1000° R). References 15 and 16 present the cold flow thrust and pumping characteristics of a promising film cooling concept using ram air.

The convectively cooled plug nozzle of reference 11 was modified to increase the partial film cooled length and was tested on an afterburning J-85 turbojet engine. The heat transfer results are the subject of this report. The modification consisted of locating a slot at a position 42 percent of the distance from the nozzle throat to the plug tip. Thus, 42 percent was convectively cooled and the remainder was film cooled. Tests were conducted over a range of nozzle inlet pressures from 5.5 to 19.4 newtons per square centimeters (8 to 28 psia), pressure ratios from 2 to 30, coolant flow rates from 0.04 to 1.13 kilograms per second (0.1 to 2.5 lb/sec), and exhaust gas temperatures from 1330 to 2040 K (2400° to 3675° R). The coolant flow was supplied from a facility source at ambient temperatures.

Cooling characteristics are presented as plots of plug surface temperature and pressure distributions. The coolant pressure-flow characteristics are described by the

coolant to primary total pressure ratio as a function of the ratio of corrected coolant to primary weight flow ratio. The effect of independent variations in nozzle flow rate, temperature, nozzle pressure ratio, and coolant flow rates are shown. Data showing the effect of nozzle outer shroud length are also presented. Comparisons of the film cooled performance with that of the truncated convectively cooled configuration are made. A list of symbols used in the report are included in the appendix.

APPARATUS

Engine Installation

The partial film cooled plug nozzle was mounted on a General Electric J85-13 turbojet and installed in the Lewis Research Center altitude facility (PSL 2). The installation is shown pictorially in figure 1 and schematically in figure 2. The J85-13 engine has an eight-stage axial flow compressor, an annular primary combustor, a two-stage axial flow turbine, and an afterburner with a single circumferential V-gutter flameholder and radial fuel spray bars. At sea-level static conditions the rated airflow is 20 kilograms per second (44 lb/sec) at an engine pressure ratio of about 2.2. At maximum afterburning the exhaust gas temperature is about 2000 K (3600° R).

The altitude facility has the capability of operating over a range of altitudes from sea level to 24 000 meters (80 000 ft) at corresponding air flows from 218 to 5 kilograms per second (480 to 10 lb/sec). A range of exhaust nozzle pressure ratios with afterburning from about 2 to 30 were possible.

The engine was mounted on a thrust measuring stand which consisted of a test bed suspended from four facility support flexure rods. The altitude chamber includes a forward bulkhead which separates the inlet plenum from the test chamber. Atmospheric air was supplied to the plenum at the desired pressure by control valves and flowed from the plenum through the direct connect bellmouth and duct to the engine inlet.

The exhaust gases from the engine were captured by a collector, which extended through the rear bulkhead, to minimize recirculation of these gases into the test chamber. The exhaust pressure was controlled by valves in the exhaust system.

Plug Nozzle

General description. - A closeup view of the plug nozzle installed in the facility is presented in figure 3. The principal parts of the plug nozzle system are illustrated by the schematic diagram of figure 4 and consist of the plug, the primary shroud, an outer shroud, and the supporting struts. The maximum diameter of the plug is 40.64 centime-

ters (16 in.) and the plug cone forms a 10^{o} half angle.

The plug was supported from the outer shroud by three struts. The struts were elliptical with a major axis of 14 centimeters (5.5 in.) and a minor axis of 6.3 centimeters (2.5 in.). Two lengths of outer shroud were used during this investigation to simulate a high and a low internal area ratio obtainable with a variable outer shroud length. Ideally, there is an optimum shroud length for each operating nozzle pressure ratio for maximum thrust.

The two outer shroud lengths used are shown in figure 4. The short shroud terminated at a point 12.7 centimeters (5 in.) (X/D_m = -0.2) upstream of the nozzle throat. The long shroud extended to a point 38.1 centimeters (15 in.) (X/D_m = +0.6) downstream of the nozzle throat. The diameter D_m of the outer shroud was 63.5 centimeters (25 in.).

The forward end of the primary shroud was connected to the afterburner through a packing (hot gas slip seal shown in fig. 4) to allow for differential thermal expansion between the nozzle and the afterburner. The lip at the aft end of the primary shroud formed the throat of the nozzle. It provided a throat area of about 1129 square centimeters (175 in.^{2}) and permitted operation at maximum afterburning.

Cooling system. - The various parts of the nozzle were cooled by four metered air streams supplied from the facility at ambient temperature. The flow paths for these coolant streams are shown in figure 5. The secondary air stream film cooled the outer shroud. The amount of corrected secondary weight flow ratio was held constant at 6 percent of the primary flow. The primary shroud was film cooled by two separate air streams supplied to two slots in the shroud. The primary shroud cooling air flows were each held constant at approximately 1 percent of primary flow. The forward portion of the primary shroud was film cooled by turbine discharge gas exiting from between the afterburner liner and casing.

The strut and plug cooling air stream was one of the major variables in the investigation. The struts and the front portion of the plug to a point 42 percent of the length from the throat to the theoretical tip of an uncooled plug (fig. 5) was convectively cooled. The remaining downstream portion of the plug was film cooled. All the film cooling results presented in this report are with a nontruncated plug, although a truncation junction at a plane 60 percent of the length from the throat existed in the assembly.

Details of the convectively cooled portion of the plug and the struts are described in references 9 and 10. The film cooled portion of the plug was formed by cutting off a section of the plug and welding on a slot and cone extension assembly. Figure 5 shows the details of the slot design. Basically, it was a slot forming a rearward facing step in the surface of the plug that discharged the coolant stream tangentially to the surface. The slot assembly consisted of 64 equally spaced fins which were shaped to form convergent-divergent passages. Since the slot was located in a supersonic hot gas stream, the objective at design point conditions was to obtain supersonic discharge velocities from the

slot. Ideally, to obtain the maximum insulating effect of the coolant stream, the velocity of the coolant stream should be matched with the primary stream to minimize mixing (ref. 17). To achieve this condition, however, a large exit to throat area ratio in the slot was required which resulted in too high a pressure inside the plug. Therefore, as a compromise, the slot was designed for the maximum Mach number M possible, consistent with the available pressure supply inside the plug. This resulted in a design point value of $M = 1.80$ at the coolant slot exit compared to a primary stream $M = 1.36$ at the slot station. The physical flow area at the exit of the slot was 40 square centimeters (6.20 in.^{2}) and the exit-to-throat physical area ratio was 1.5.

Instrumentation

The results presented in this report were obtained from measurements made with instrumentation summarized in figure 6. Additional instrumentation was available at the start of the tests but were lost during testing; these are not shown in the figure.

In addition to the instrumentation on the plug wall, there were two pressure taps inside the plug p_c, two thermocouples T_{ce}, (air temperature) and two static pressure taps p_{sc}, in the coolant passage at the entrance to the slot assembly, and a static pressure tap just inside the exit of the slot. These measurements were used in determining the pressure-flow characteristics of the cooling systems.

The exhaust pressure p_0 of the nozzle was measured by four static pressure tubes equally spaced around the outside surface and near the end of the outer shroud.

The gas stream total pressure at the inlet to the nozzle P_p was measured at station 7 (fig. 4) with a water-cooled pressure rake. The rake had ten elements, two at each of five radii, and positioned so that they were equal area weighted.

The temperature at the inlet to the nozzle was not measured but instead determined from a correlation of the temperature rise in the afterburner with the parameter $(P_5)^2/W_5$ and the afterburner fuel-air ratio. The correlation was derived from calibrations previously obtained from tests with water-cooled sonic nozzles.

The exhaust temperature T_p was then obtained from a heat balance considering the primary shroud coolant flows and the leakage through the hot gas seal. The hot seal leakage was determined from a heat balance in the secondary flow passage.

TEST PROCEDURE

The facility air control valves permitted independent variation of engine inlet and altitude exhaust pressures such that nozzle pressure ratio could be varied independently of engine inlet airflow and pressure level. The primary exhaust gas temperature was

also independently variable by different levels of afterburning. The other independent variable having a significant effect on nozzle cooling was the plug cooling air flow rate. Thus, the four major independent test variables in addition to configuration changes are: (1) primary air flow, (2) nozzle pressure ratio, (3) coolant flow rate, and (4) exhaust gas temperature.

Test conditions were selected so that the independent effect of each of the major variables could be obtained. Three of the test variables were held constant while the fourth was changed. The data presented in this report were for selected test points obtained within the matrix of test conditions presented in table I.

RESULTS AND DISCUSSION

The results from selected typical runs are presented to show the effect of nozzle pressure ratio, coolant flow rate, and nozzle primary flow rate (nozzle inlet pressure) on the temperature and pressure distributions on the plug at maximum afterburning conditions, where cooling is most difficult. Results are also included to show the effect of reducing the exhaust gas temperature and the effect of outer shroud length.

A comparison is made with the all convectively cooled plug design of reference 9. Finally, the coolant pressure-flow (pumping) characteristics are compared with the all convectively cooled design to show the reduction in supply pressure that can be achieved by the partial film cooled design.

Temperature and Pressure Distributions

Effect of nozzle pressure ratio. - The effect of the nozzle pressure ratio P_p/p_0 on the temperature and pressure distributions on the surface of the plug is shown in figure 7. The temperatures shown (fig. 7(a)) are the measured wall temperatures uncorrected for radiation or heat loss through the wall. The wall static pressures and exhaust pressure p_0 are shown (fig. 7(b)) as ratios to the total pressure P_p at the entrance to the nozzle (station 7). Both temperatures and pressures are plotted as a function of the distance Y along the surface of the plug as a ratio to the length L from the front end to the truncation junction. Ratios greater than 1.0 are therefore locations on the conical extension to a full length plug. This dimensioning method was chosen to make the results readily comparable with those of reference 9. The test conditions for all data in figure 7 were: exhaust gas temperature of 2030 K (3650° R), nozzle inlet pressure of 19.3 newton per square centimeter (28 lb/in.^{2}), and a coolant flow ratio W_c/W_p of 0.026.

With the nozzle operating at a pressure ratio of 9.85, the wall temperature (fig. 7(a)) on the convectively cooled portion of the plug decreased uniformly from a maximum of 1110 K (2000° R) near the throat (Y/L = 0.43) to a low temperature of 830 K (1500° R) at the slot. The solid symbols are the highest (peak values) of the seven individually measured temperatures around the circumference at the throat. Immediately downstream of the exit of the slot (Y/L = 0.82), the wall temperatures showed a decided drop due to the effect of the film of air exiting from the cooling air slot which was followed by a slowly rising wall temperature in the downstream direction. At the truncation junction (Y/L = 1.0), the temperature dropped because of leakage at the joint and then began to rise sharply. (The dashed curves represent the probable characteristic if no leak were present.)

A maximum wall temperature of about 944 K (1708° R) was measured near the midpoint of the extension which was substantially less than the 1200 K (2200° R) design wall temperature. It was, therefore, concluded that at a nozzle pressure of 10 (or higher) a coolant flow of 2.6 percent of primary flow was more than sufficient to keep the entire plug nozzle surface cool.

The wall static pressures on the convectively cooled portion (fig. 7(b)) decreased uniformly from the throat to the slot. This is a favorable pressure gradient and exists along the surface from the smoothly expanding gases. Downstream of the slot, the pressure, also influenced by the cooling air film, increased to a slightly higher constant level over the length to the truncation junction. Downstream from the junction, the measured wall static pressure gradient became adverse from shock waves forming.

As the nozzle pressure ratio was decreased, the shock waves moved upstream. The adverse pressure gradients associated with the shocks, also moved upstream and the temperatures on the surfaces (both convective and film cooled) increased along with them. The adverse gradient for a pressure ratio of 5.1 started between Y/L = 0.53 and 0.67 and remained adverse up to Y/L = 0.87. A weak adverse gradient was observed farther downstream at values of Y/L = 0.98 to 1.11. Undoubtedly, the presence of adverse gradients increased the turbulent mixing of hot gas into the film cooling air and caused the wall temperature of the film cooled portion of the plug to be higher than for the 9.85 pressure ratio previously discussed. For a pressure ratio of 2.9, the presence of three shock waves along the length of the plug were indicated by three adverse pressure gradients plotted in figure 7(b). The combined effect of the three shocks, although each occurs over a relatively short extent but exhibiting high pressure amplitude, disturbed the film cooling such that the wall temperature is nearly as high for the 5.1 pressure ratio data. These data indicate that film cooling effectiveness is strongly influenced by the extent and amplitude of adverse pressure gradients resulting from shock waves. The exhaust collector was positioned far enough downstream (fig. 1) so that it had no effect on pressure distributions and shock positions along the plug for the data in this report.

The wall temperature level of the convectively cooled surface was highest at a nozzle pressure ratio of 3. At pressure ratios of both 2.9 and 5.1, peak temperatures of 1110 K (2000° R) occurred at both the throat and the slot. As expected, high temperatures occurred at the throat due to high heat loads at this minimum flow area of the nozzle. The peak temperature at the slot is the result of the shock (indicated by the adverse pressure gradient) also affecting the convection heat transfer.

For the test condition of $P_p/p_0 = 5.1$, the limiting temperature of 1220 K (2200° R) was reached at about the midpoint of the film cooled cone extension. A coolant flow of about 2.6 percent of the engine flow was sufficient to cool the film cooled plug up to the 60 percent truncation junction, but not enough to keep the full length extension within design limits. These results show that cooling the plug was most difficult at nozzle pressure ratios below 10 for both convection and film cooling.

Effect of coolant flow rate. - The effect of coolant flow rate is shown in figure 8 for a nozzle pressure ratio of 5. With the exhaust gas temperature and the inlet pressure set at the maximum values investigated, the coolant flow was set at 2.6, 4.6, and 5.7 percent of primary flow. The characteristic shape of the temperature distributions (fig. 8(a)) remained unchanged for all coolant flows, and, as expected, the level decreased as flow rate increased. The variation in coolant flow also had very little effect on pressure distributions (fig. 8(b)). It is obvious from figure 8 that a coolant flow rate of approximately 2.6 percent would be insufficient to adequately cool the extended film cooled surface for this pressure ratio condition.

A cross plot of the data from figure 8 is presented in figure 9 to show the variation of wall temperature (at selected values of Y/L) with coolant flow rate. Assuming that the extrapolations to lower coolant flows are valid, the results show that a coolant flow of 1.8 percent of primary flow would keep the film cooled portion of the truncated plug and the slot outer wall under 1220 K (2200° R). This flow rate is also considered adequate to cool the throat region of the plug (Y/L = 0.372 in fig. 9). It should be pointed out, however, that these results are with the coolant supplied to the nozzle at ambient temperature. If the coolant were to be supplied at compressor discharge temperatures, higher flow rates would be required.

Effect of hot gas flow rate (inlet pressure). - The effect of hot gas flow rate on wall temperature and pressure distributions is presented in the curves of figure 10. The flow rate and nozzle inlet pressure both vary with engine test conditions. The nozzle pressure ratio was the same for the three test points shown. Although the hot gas temperature and coolant flow rates are not exactly matched, the effect of the differences tend to cancel each other such that the maximum wall temperatures of the convectively cooled portion are within about 28 K (50° R) of each other. Both the temperature and pressure distributions along the plug surface show the same trends which are independent of the hot gas flow rate and the corresponding nozzle inlet pressure.

Effect of coolant flow rate at lower hot gas temperatures. - The results of tests conducted at a lower hot gas temperature of about 1350 K (2430° R) over a range of coolant flow rates is presented in figure 11. The resulting temperature and pressure distributions indicate that very low (perhaps zero) coolant would be adequate to maintain allowable temperatures for the plug at a nozzle pressure ratio of 3.2.

Effect of shroud length. - Change in length of the outer shroud changes the internal area ratio of the nozzle and thus the axial velocity distribution of the expanding hot gas flowing along the plug surface. Comparisons of temperature and pressure distributions along the plug surface for the short and long shrouds tested are presented in figure 12 ($P_p/p_0 = 10$) and figure 13 ($P_p/p_0 = 3$).

Two data points are shown in figure 12 where the test conditions are nearly the same, but the shroud lengths are different which changed the position of the shock along the plug surface. An adverse pressure gradient began at $Y/L = 0.66$ (within the convectively cooled portion) for the long shroud configuration and at the slot $Y/L = 0.82$ for the short shroud configuration. The wall temperature started climbing at the beginning of the adverse pressure gradient in both cases, whether in the convectively cooled portion (long shroud) or in the film cooled portion (short shroud) of the plug. Downstream of the film cooling slot on the long shroud configuration, however, the pressure gradient is favorable and the film cooled wall temperature remained nearly constant (ignoring the effect of the small leakage at $Y/L = 1$). The level of the film cooled wall temperature near the slot is higher for the long shroud than for the short shroud indicating that, even though the pressure gradient is locally favorable, the presence of the upstream shock affected the film cooling of the surface downstream of the slot. For the short shroud data, the adverse gradient persisted throughout the length of the film cooled surface which resulted in a rapid continual rise in wall temperature in the downstream direction. These data reinforce the discussion of figure 7 with respect to adverse pressure gradients having a pronounced effect on film cooling whether the adverse gradient is within a film cooled portion or upstream of it.

The effect of shroud length for tests with a lower pressure ratio ($P_p/p_0 = 3$) is shown in figure 13. The difference in pressure distributions is small (the long shroud is probably operating with unattached flow). The small difference (55 K (100° R)) in wall temperatures is probably due to the slightly higher pressure amplitude of the adverse pressure gradients for the long shroud configuration.

Comparison with all convection cooling. - Figure 14 shows a comparison of the temperature and pressure distributions on the full length partially film cooled plug with those from the truncated all convective cooled design of reference 9. Data from three test points are presented. The first two (circular and square symbols in fig. 14) compare the partial film cooled plug data with the all convection cooled plug data (test points previously unpublished) where the cooling air is supplied from the facility system at 314 K (565° R). Again, the hot gas temperature and coolant flow rates are not exactly

matched but the effect of the differences tend to cancel each other such that the resulting plug wall temperature (fig. 14(a)) of the two cases for $Y/L < 0.8$ (convective cooled portion) are within 28 K (50° R). The film cooled portion is 90 to 150 K (160° to 250° R) cooler than the all convection cooled design up to the truncation junction at $Y/L = 1.0$.

The third test in figure 14 (triangular symbols) shows data for the all convection cooled plug (data previously unpublished) with cooling air being supplied from the engine compressor discharge (customer bleed ports) at a temperature of 509 K (916° R), approximately 193 K (350° R) higher than for the other tests just described. The plug wall, hot gas, and coolant exit temperatures for this test were about the same as for the other all convection cooled test with facility air supply. It required an additional 1.2 percent cooling air, however, because of the higher coolant supply temperature. In the discussion of figure 9, it was estimated that 1.8 percent coolant would be sufficient to cool the truncated film cooled portion using facility air. With the cooling air being supplied at the higher temperature of 509 K (916° R), and assuming the same trend as shown in figure 14, it is estimated that an additional 1.2 percent in coolant flow (a total of 3.0 percent) would be required to cool a partial film cooled plug truncated at 60 percent of the length using compressor air. This represents a 14 percent reduction in cooling air requirement compared to the all convectively cooled plug, which required 3.5 percent of compressor air flow (ref. 9).

The pressure distributions shown in figure 14(b) are nearly the same for the convectively and film cooled configurations up to the slot station. The presence of the slot and film cooling air flow affects the pressures downstream of the slot on the partial film cooled design. The lower pressure (and temperature) at $Y/L = 1.0$ for the customer bleed test (triangular symbol) is due to use of the short outer shroud for this test; the other two tests were with a long outer shroud. (The effect of shroud length was discussed in the previous section.)

Coolant Pressure-Flow Characteristics

The data shown in figure 15 compares the pressure-flow characteristics (pumping characteristics) of the partially film cooled plug design with the all convectively cooled design (ref. 9) obtained during engine tests. In figure 15(a) the variation of the ratio of coolant slot total pressure to exhaust gas total pressure with corrected coolant weight flow ratio is shown, and in figure 15(b) the ratio of plug interior pressure (total pressure) to exhaust gas total pressure is plotted. For the convectively cooled configuration both curves are based on measured total pressures. For the partially film cooled configuration, the total pressure at the slot is calculated from static pressure, total temperature, and flow rate at the inlet to the convergent-divergent slot configuration.

The pumping characteristics can be analytically expressed by the following equation which is derived from the continuity equations written for the flow at the throat of the coolant passage and the flow at the throat of the primary, both with choked flow:

$$\frac{W_c}{W_p}\sqrt{\frac{T_{ce}}{T_p}} = \left(\frac{P_{ce}}{P_p}\right)\left(\frac{A_c}{A_p}\right)\left[\frac{f(\gamma_c)}{f(\gamma_p)}\right] \tag{1}$$

where

$$f(\gamma) = \frac{\sqrt{\gamma g}}{\left(\frac{\gamma+1}{2}\right)^{(\gamma+1)/2(\gamma-1)}}$$

For each design, if A_c/A_p and $f(\gamma_c)/f(\gamma_p)$ remain constant with change in corrected coolant weight flow ratio, the relation between the coolant flow ratio and the total pressure ratio P_{ce}/P_p is linear. The slope is predominantely dependent on the ratio of throat sizes A_c/A_p. (The effect of $f(\gamma_c)/f(\gamma_r)$ is small.) The test results plotted in figure 15(a) show the linear relation, and the difference in the slopes of the two data sets represents the difference in the exit throat areas of the two cooling methods.

The total pressure ratio P_{ce}/P_p may be written as

$$\left(\frac{P_{ce}}{P_p}\right) = \left(\frac{P_c}{P_p}\right)\left(\frac{P_{ce}}{P_c}\right) \tag{2}$$

Substituting equation (2) into equation (1) yields

$$\frac{W_c}{W_p}\sqrt{\frac{T_{ce}}{T_p}} = \left(\frac{P_c}{P_p}\right)\left(\frac{P_{ce}}{P_c}\right)\left(\frac{A_c}{A_p}\right)\left[\frac{f(\gamma_c)}{f(\gamma_p)}\right] \tag{3}$$

If the total pressure loss in the coolant passage P_{ce}/P_c is constant, the coolant flow rate should be a linear function of P_c/P_p. These values for each configuration are plotted in figure 15(b) and show the relation to be linear. The slopes of the curves in figure 15(b) are then a combined function of both the pressure loss and the ratio of throat areas. The change in slope between figures 15(a) and (b) for each configuration then represents the total pressure loss in the coolant passage in each configuration.

For the all convectively cooled plug design, from figure 15 it is found that the total pressure loss in the coolant passage is 25 percent of the total pressure inside the plug.

For the partially film cooled plug design, the total pressure loss is 13 percent or almost a 50 percent reduction. The supply pressure then could be reduced an equivalent amount. Coolant supply pressure requirements have a significant effect on choice of source of cooling air which in turn affects the engine cycle penalties (see ref. 12).

SUMMARY OF RESULTS

An air-cooled plug nozzle with the forward portion convectively cooled and the aft portion film cooled was tested on a J-85 afterburning turbojet in an altitude test chamber to determine the amount of air and supply pressure needed to cool the plug wall to below 1220 K (2200° R) at a maximum afterburning temperature of 1940 K (3500° R). In the configuration tested, a tangential annular slot was located on the plug about 42 percent of the distance from the throat to the tip. The tests were conducted over a range of coolant flow rates and nozzle pressure ratios at various nozzle inlet pressures and temperatures. The coolant flow was supplied from a facility source at ambient temperature. The significant results were as follows:

1. Comparing the results with an all convectively cooled plug nozzle truncated at 60 percent length, equal amounts of coolant flow resulted in wall temperatures that were from 90 to 150 K (160° to 250° R) lower on the film cooled portion of a partial film cooled plug of the same length.

2. Converting the all convectively cooled truncated plug to a partially film cooled plug reduced the loss of total pressure in the plug coolant passages from 25 to 13 percent, almost a 50 percent reduction.

3. The wall temperature distributions for both convective and film cooled portions of the plug tested were strongly influenced by shock waves which produce adverse pressure gradients along the plug surface.

4. Film cooling of the plug was more difficult at nozzle pressure ratios below 10.

5. From extrapolating the results of varying the coolant flow at a nozzle exhaust temperature of 2040 K (3670° R), nozzle inlet pressure of 19.3 newtons per square centimeter (28 psia), a nozzle pressure ratio of 5, and using ambient temperature cooling air, the plug cooling flow required to keep maximum wall temperatures under 1220 K (2200° R) would be:

   (a) 1.8 percent for a 60 percent truncated plug

   (b) 2.6 percent for a nontruncated plug

6. An estimated cooling air flow rate of 3.0 percent of compressor discharge would be needed to cool a 60 percent truncated partially film cooled plug. This is about a 14 percent reduction in cooling air from that required for an all convectively cooled plug of the same length.

7. At an exhaust temperature of 1330 K (2400° R), practically no coolant flow would be needed to keep all surface temperatures under 1220 K (2200° R).

Lewis Research Center,
National Aeronautics and Space Administration,
Cleveland, Ohio, December 12, 1975,
505-04.

APPENDIX - SYMBOLS

A_c	coolant slot throat area
A_p	primary nozzle throat area
D_m	outer shroud diameter (model diameter)
g	gravitational constant
L	length along plug surface, front end to truncation station
M	Mach number
P_c	coolant total pressure inside plug
P_{ce}	coolant slot exit total pressure
P_p	nozzle primary inlet total pressure
P_5	turbine exit total pressure
p_{sc}	coolant slot inlet static pressure
p_w	plug wall static pressure
p_0	exhaust pressure at nozzle exit
T_{ce}	coolant slot exit total temperature
T_{ci}	coolant inlet total temperature
T_p	nozzle primary total temperature
T_w	plug wall temperature
W_c	coolant weight flow rate
W_p	primary weight flow rate
W_5	turbine exit weight flow rate
X	length of outer shroud from primary throat
Y	length along plug surface from front end
γ	specific heat ratio
γ_c	coolant specific heat ratio
γ_p	primary specific heat ratio
θ	angular position

REFERENCES

1. Bresnahan, Donald L.; and Johns, Albert L.: Cold Flow Investigation of a Low Angle Turbojet Plug Nozzle with Fixed Throat and Translating Shroud at Mach Numbers from 0 to 2.0. NASA TM X-1619, 1968.

2. Bresnahan, Donald L.: Experimental Investigation of a 10^{o} Conical Turbojet Plug Nozzle with Iris Primary and Translating Shroud at Mach Numbers From 0 to 2.0. NASA TM X-1709, 1968.

3. Bresnahan, Donald L.: Experimental Investigation of a 10^{o} Conical Turbojet Plug Nozzle with Translating Primary and Secondary Shrouds at Mach Numbers From 0 to 2.0. NASA TM X-1777, 1969.

4. Johns, Albert L.: Quiescent-Air Performance of a Truncated Turbojet Plug Nozzle with Shroud and Plug Base Flows From a Common Source. NASA TM X-1807, 1969.

5. Harrington, Douglas E.: Performance of Convergent and Plug Nozzles at Mach Numbers from 0 to 1.97. NASA TM X-2112, 1970.

6. Harrington, Douglas E.: Performance of a 10^{o} Conical Plug Nozzle with Various Primary Flap and Nacelle Configurations at Mach Numbers from 0 to 1.97. NASA TM X-2086, 1971.

7. Huntley, Sidney C.; and Samanich, Nick E.: Performance of a 10^{o} Conical Plug Nozzle Using a Turbojet Gas Generator. NASA TM X-52570, 1969.

8. Samanich, Nick E.; and Chamberlin, Roger: Flight Investigation of Installation Effects on a Plug Nozzle Installed on an Underwing Nacelle. NASA TM X-2295, 1971.

9. Clark, John S.; Graber, Edwin J.; and Straight, David M.: Experimental Heat Transfer and Flow Results from an Air-Cooled Plug Nozzle System. NASA TM X-52897, 1970.

10. Graber, Edwin J.; and Clark, John S.: Comparison of Predicted and Experimental Heat-Transfer and Pressure-Drop Results for an Air-Cooled Plug Nozzle and Supporting Struts. NASA TN D-6764, 1972.

11. Samanich, Nick E.: Flight Investigation of an Air-Cooled Plug Nozzle with an Afterburning Turbojet. NASA TM X-2607, 1972.

12. Clark, John S.; and Lieberman, Arthur: Thermal Design Study of an Air-Cooled Plug-Nozzle System for a Supersonic-Cruise Aircraft. NASA TM X-2475, 1972.

13. Jeracki, Robert J.; and Chenoweth, Francis C.: Coolant Flow Effects on the Performance of a Conical Plug Nozzle at Mach Numbers from 0 to 2.0. NASA TM X-2076, 1970.

14. Chenoweth, Francis C.; and Lieberman, Arthur: Experimental Investigation of Heat-Transfer Characteristics of a Film-Cooled Plug Nozzle with Translating Shroud. NASA TN D-6160, 1971.

15. Straight, David M.; Harrington, Douglas E.; and Nosek, Stanley M.: Experimental Cold-Flow Evaluation of a Ram-Air-Cooled Plug-Nozzle Concept for Afterburning Turbojet Engines. NASA TM X-2811, 1973.

16. Harrington, Douglas E.; Nosek, Stanley M.; and Straight, David M.: Cold-Flow Performance of Several Variations of a Ram-Air-Cooled Plug Nozzle for Supersonic-Cruise Aircraft. NASA TM X-3110, 1974.

17. Hatch, James E.; and Papell, S. Stephen: Use of a Theoretical Flow Model to Correlate Data for Film Cooling or Heating an Adiabatic Wall by Tangential Injection of Gases of Different Fluid Properties. NASA TN D-130, 1959.

TABLE I. - MATRIX OF TEST CONDITIONS

Primary flow rate, W_p		Nozzle pressure ratio, P_p/p_0	Primary exhaust gas temperature, K (^{o}R)		
			1390 (2500)	1667 (3000)	1940 (3500)
kg/sec	lb/sec		Coolant flow ratio, W_c/W_p		
Short shroud					
19.0	42	5	----------	----------	0.02 to 0.06
		2 to 10	----------	----------	0.03
9.5	21	3	0.01 to 0.12	----------	0.02 to 0.12
5.4	12	3	----------	----------	0.01 to 0.21
		2 to 10	----------	0.01	----------
Long shroud					
19	42	15	0.01 to 0.06	----------	----------
		30	----------	----------	0.03 to 0.05
9.5	21	12	0.01 to 0.11	0.01 to 0.11	0.02 to 0.12
		3 to 18	----------	0.02	----------
		3 to 12	----------	----------	0.03
5.4	12	10	----------	0.01 to 0.20	----------
		2 to 10	----------	0.01	----------

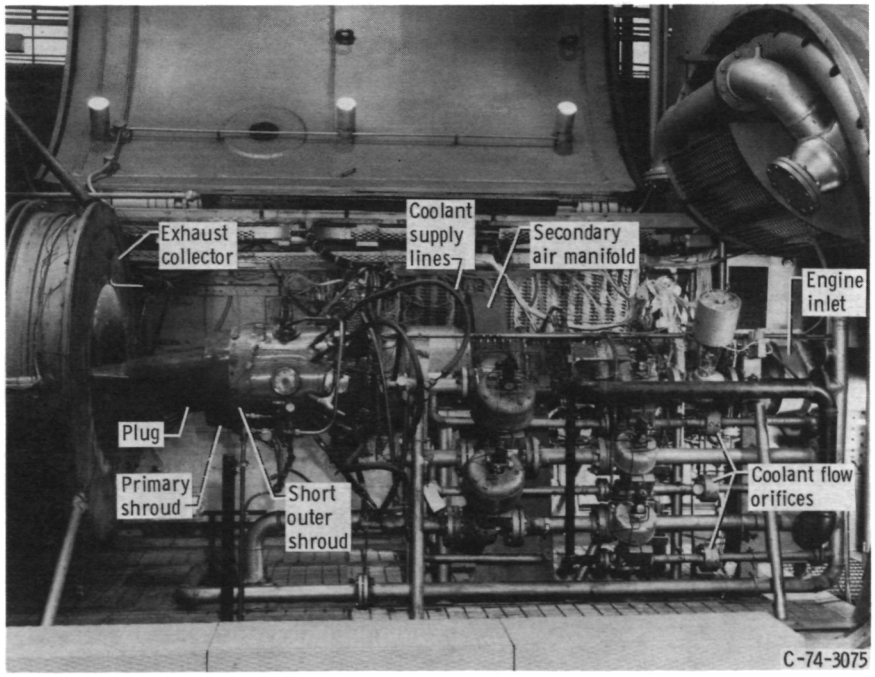

Figure 1. - Nozzle installation in test facility.

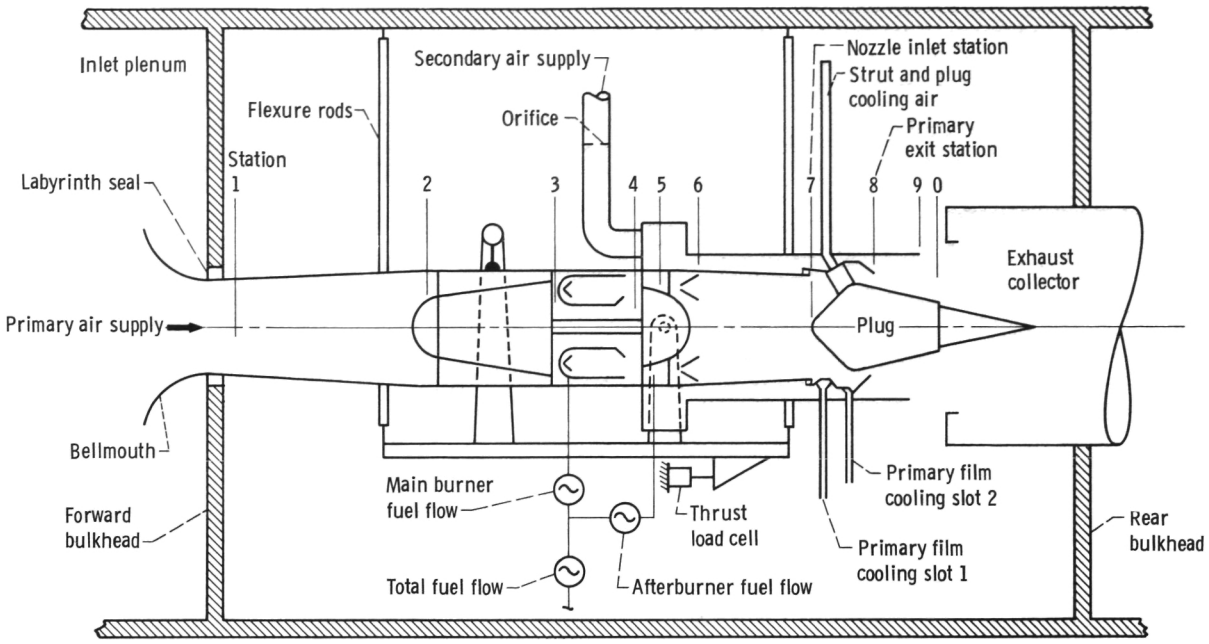

Figure 2. - Schematic of plug-nozzle test installation.

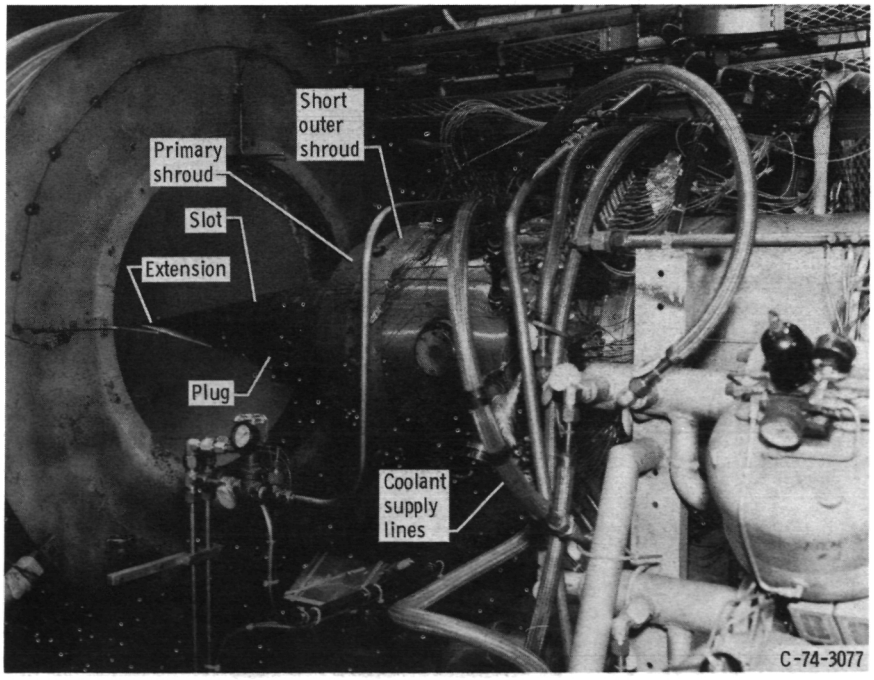

Figure 3. - Closeup of plug nozzle in test facility.

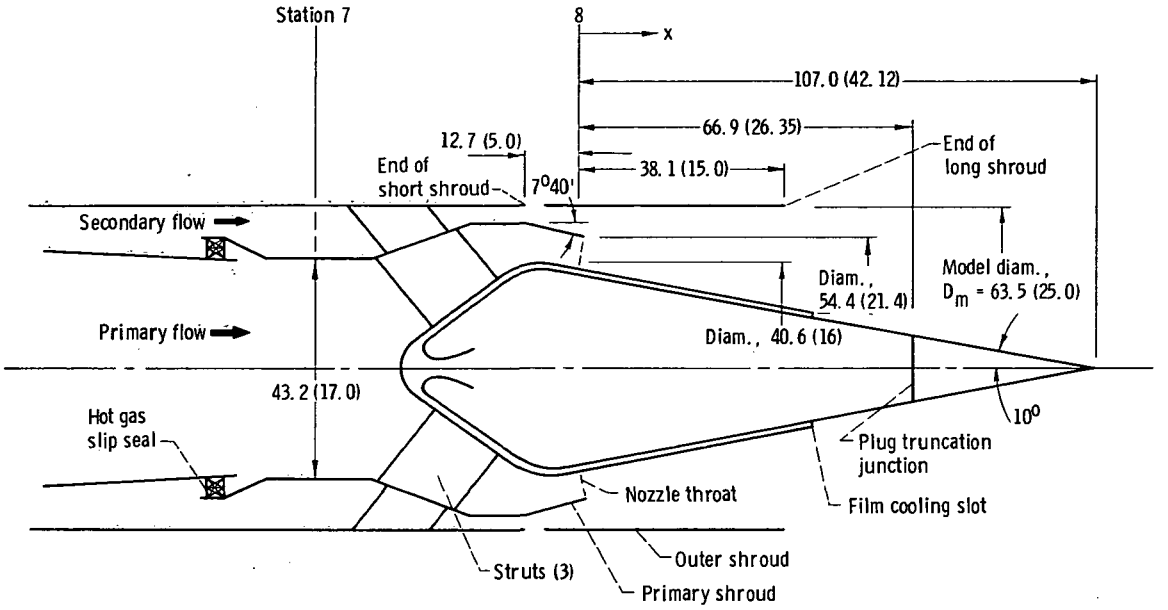

Figure 4. - Schematic of plug nozzle design. (All dimensions are in cm (in.) unless indicated otherwise.)

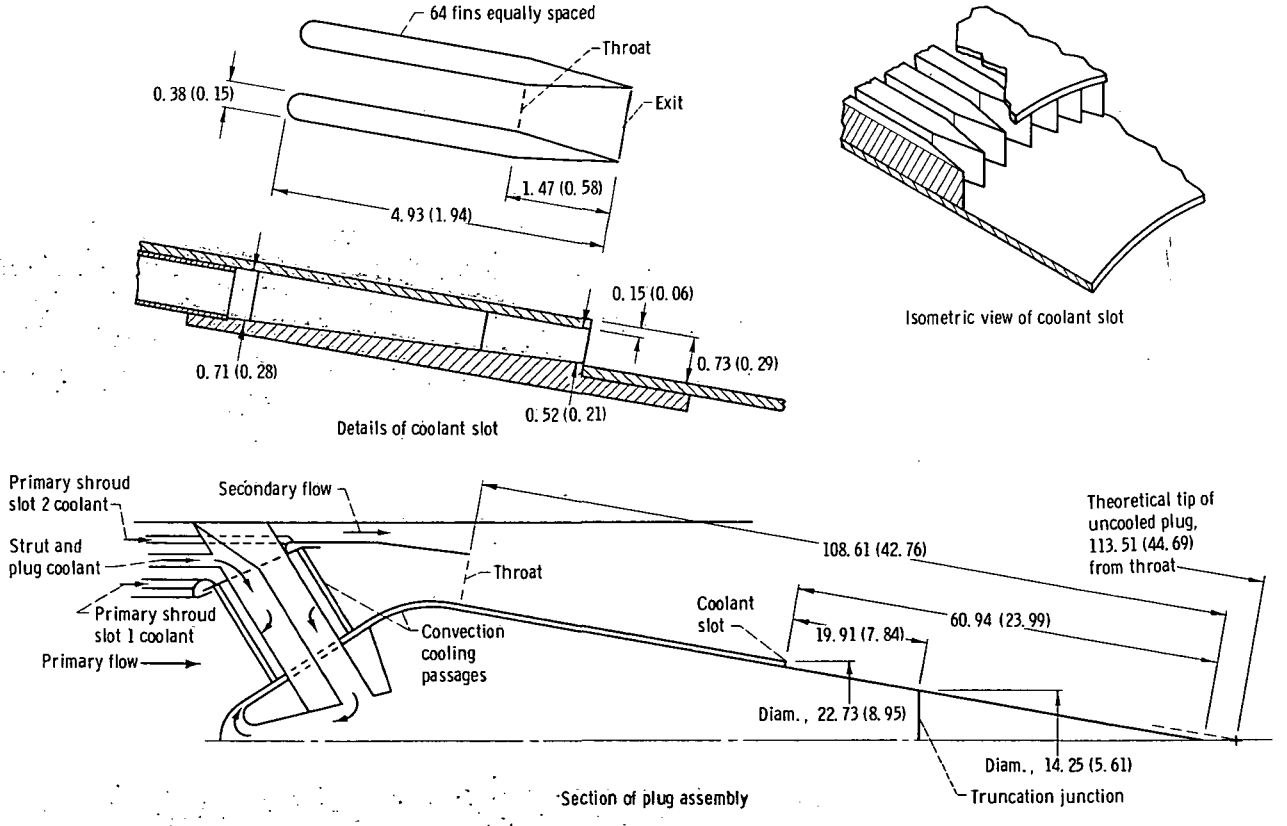

Figure 5. - Schematic and details of plug nozzle film cooling design. (All dimensions are in cm (in.).)

Thermocouple and static pressure tap locations

Y/L	T_w	p_w
	θ, [a] deg	
0.375	60	14
	90	239
	105	---
	180	---
	225	---
	270	---
	315	---
0.399	---	30
	---	225
0.431	60	45
	---	210
0.470	---	60
	---	195

Y/L	T_w	p_w
	θ, deg	
0.527	0	75
	60	180
0.661	0	90
0.756	0	105
	60	---
0.817	5	[b]165
	27	[c]175
0.837	--	0
0.848	--	0
0.872	5	0
	60	---
0.905	5	0
	30	---

Y/L	T_w	p_w
	θ, deg	
0.940	5	---
	30	---
0.973	7.5	350
1.018	60	---
1.059	60	---
1.107	0	10
	60	---
1.167	0	10

In coolant passage

Y/L	T_{ce}	p_{sc}
0.756	13	3
	73	63

[a]Clockwise looking upstream.
[b]Outside coolant slot (hot gas stream).
[c]Inside coolant slot.

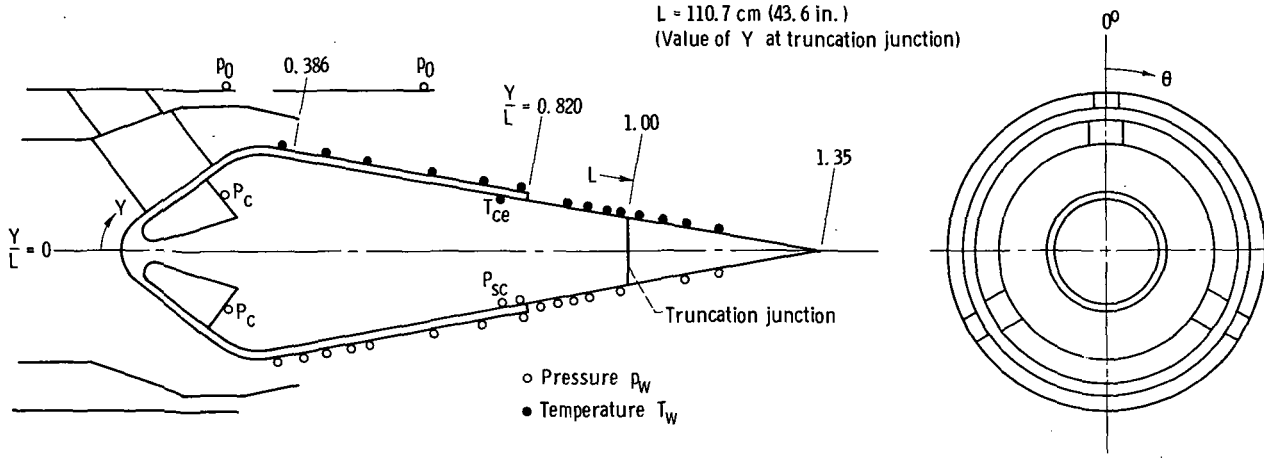

Figure 6. - Instrumentation of plug.

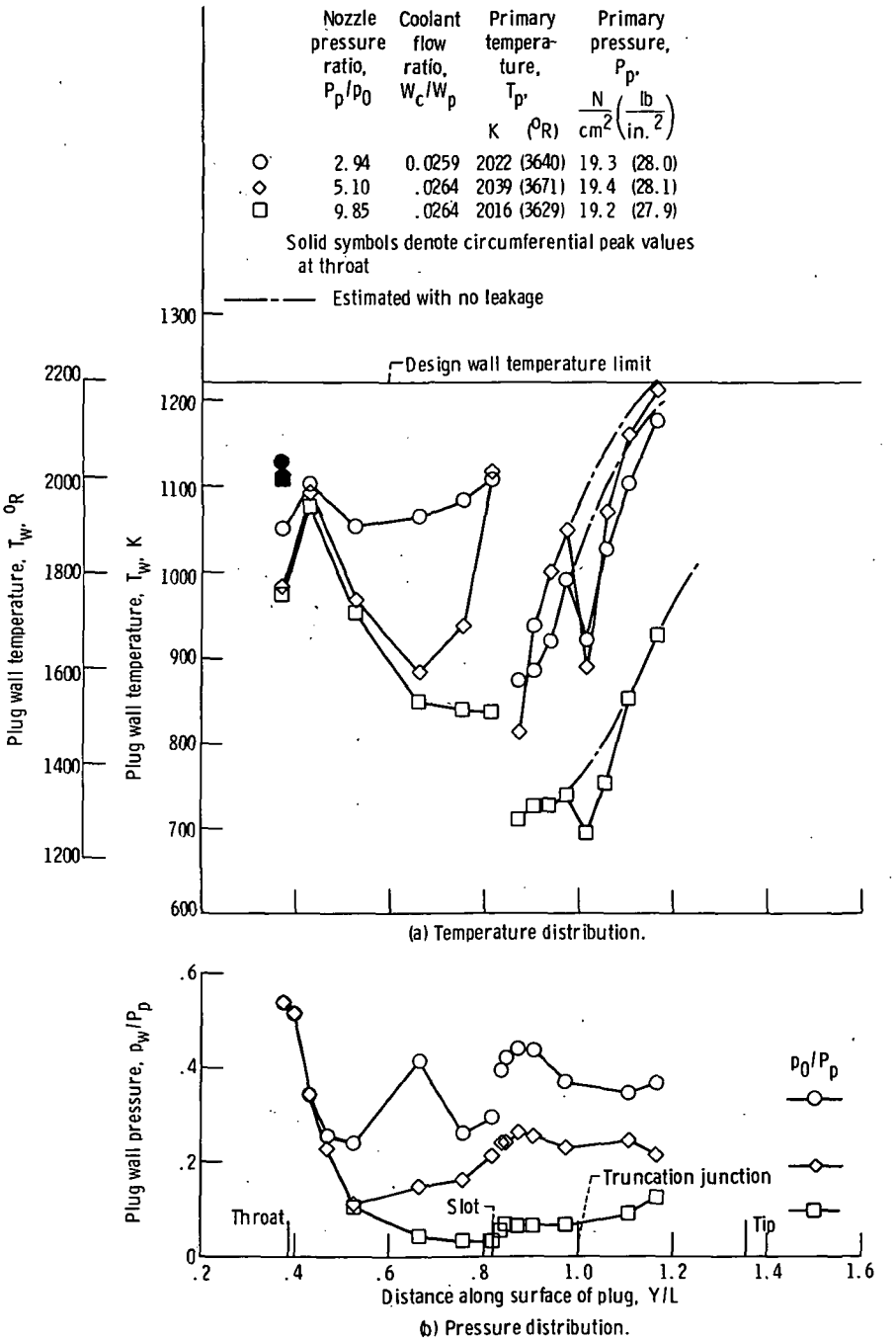

Figure 7. - Effect of nozzle pressure ratio on plug wall temperature and pressure distribution for short shroud length.

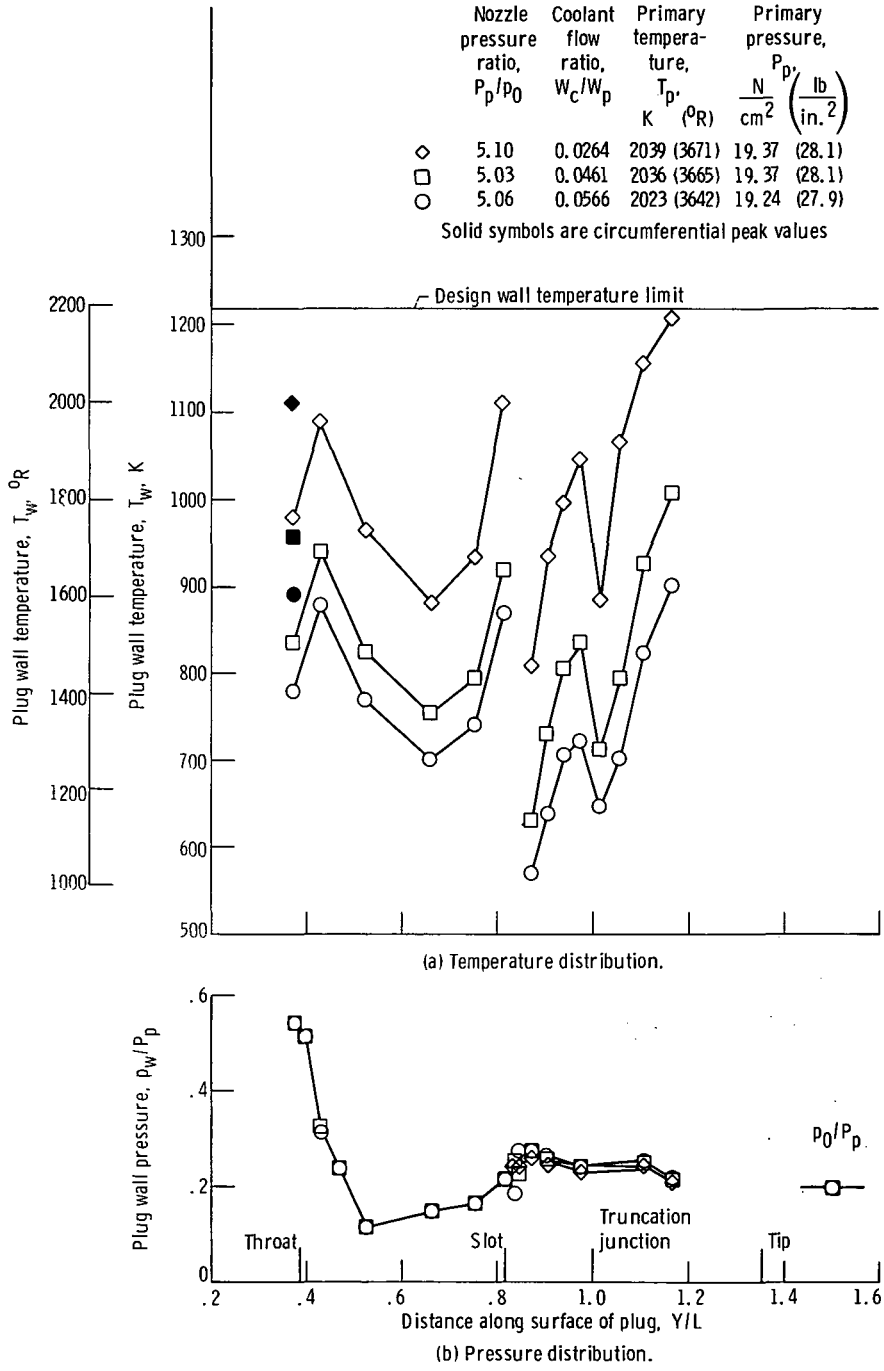

Figure 8. - Effect of coolant flow rate on plug wall temperature and pressure distributions at exhaust gas temperature of 2033 K (3660° R).

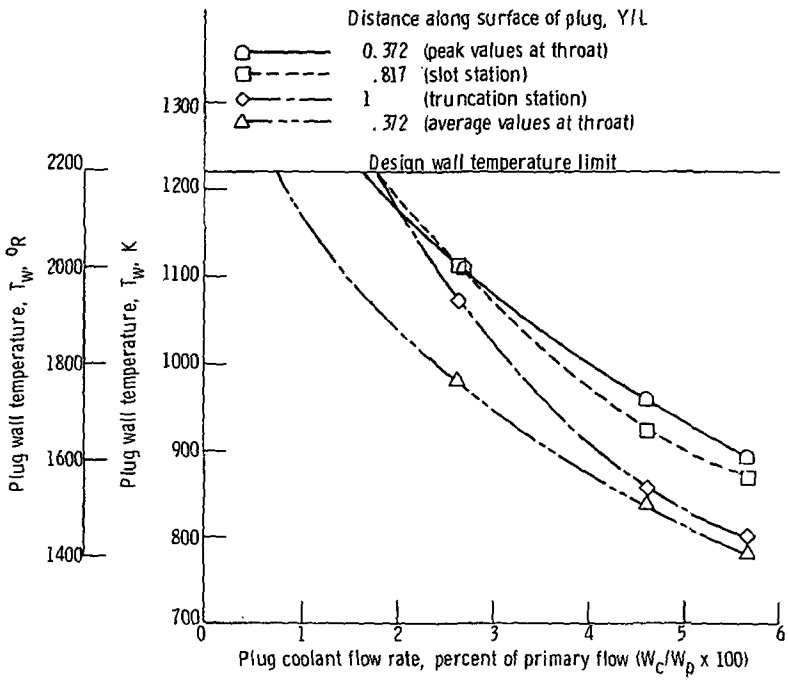

Figure 9. - Effect of coolant flow rate on temperatures at critical locations on surface of plug at primary temperature T_p = 2033 K (3660° R) and nozzle pressure ratio P_p/p_0 = 5.1.

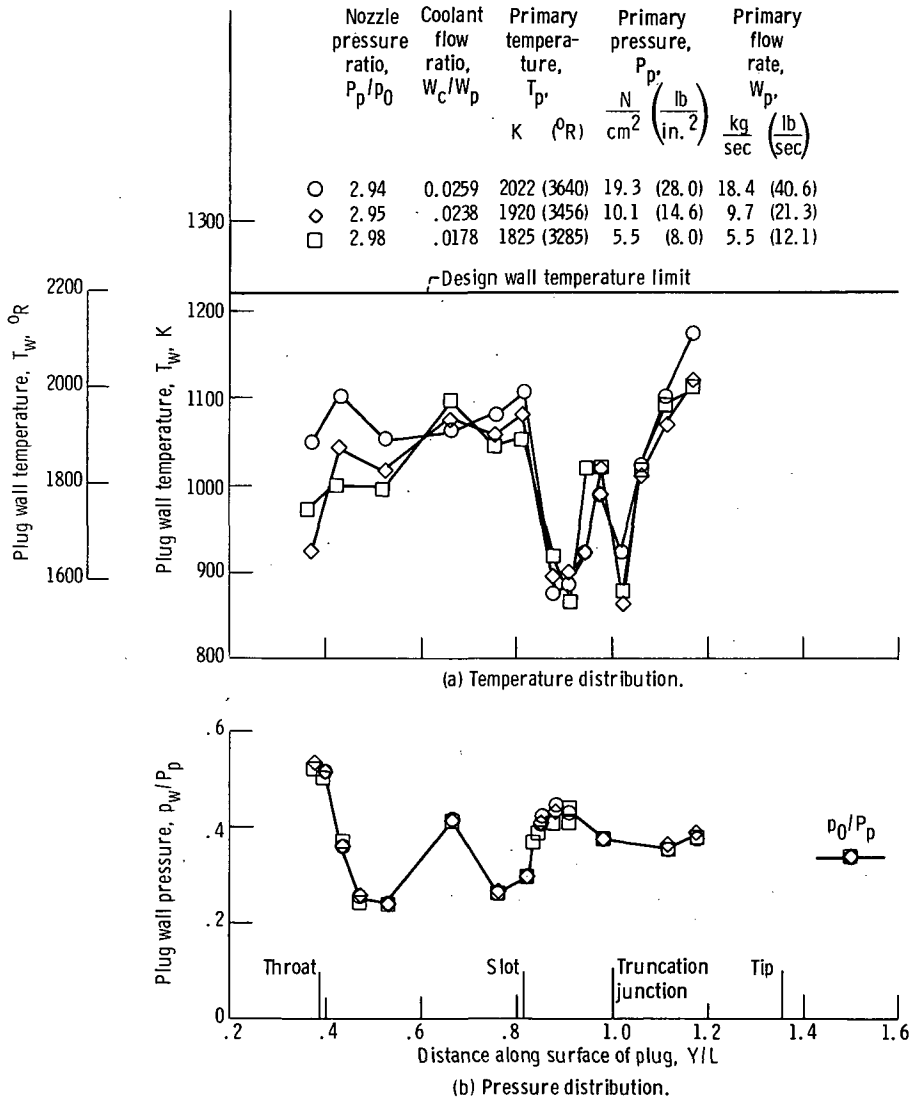

(a) Temperature distribution.

(b) Pressure distribution.

Figure 10. - Effect of nozzle primary flow rate on plug wall temperature and pressure distribution for short shroud length.

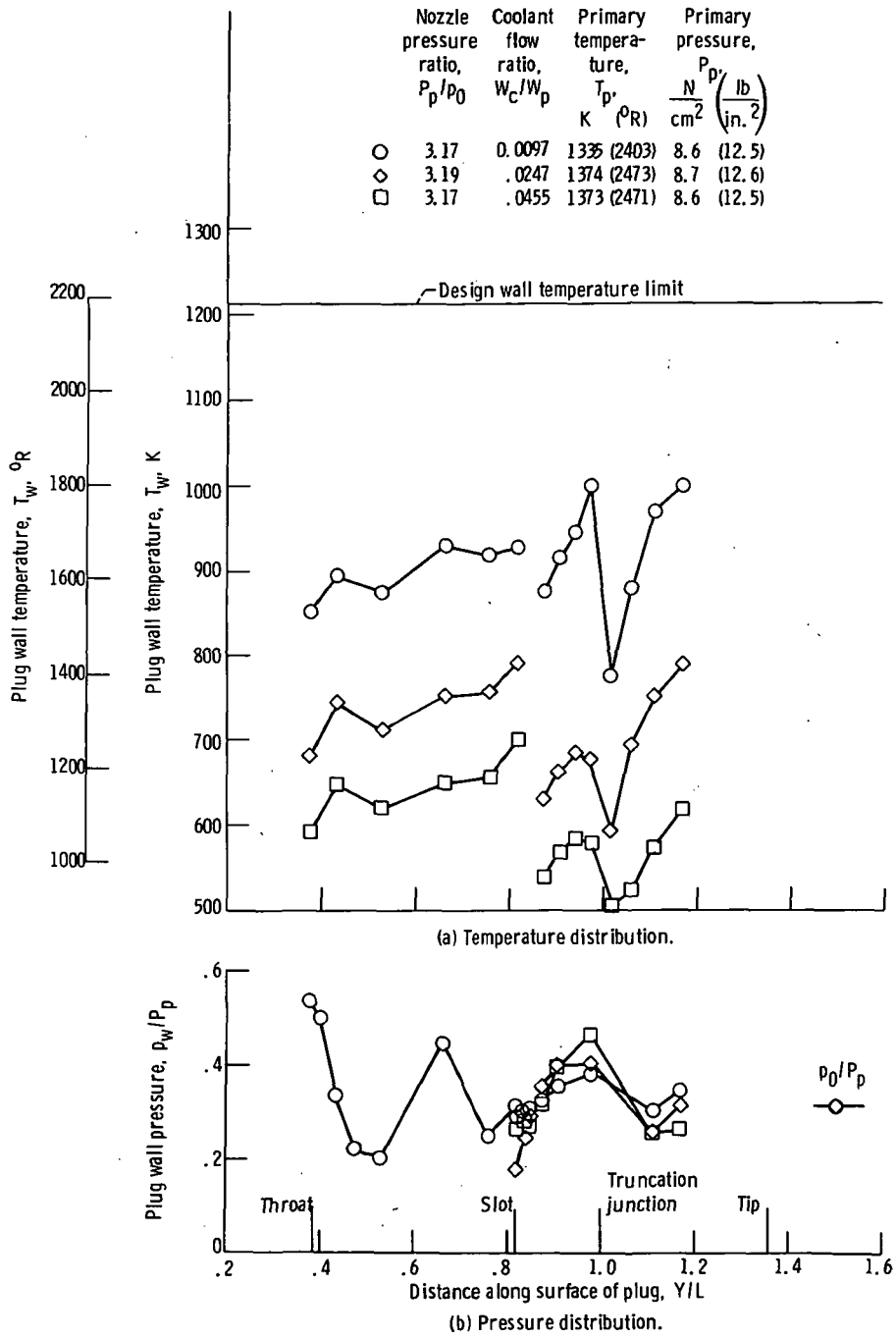

(a) Temperature distribution.

(b) Pressure distribution.

Figure 11. - Effect of coolant flow rate on plug wall temperature and pressure distributions at exhaust gas temperature of 1350 K (2430° R) for short shroud length.

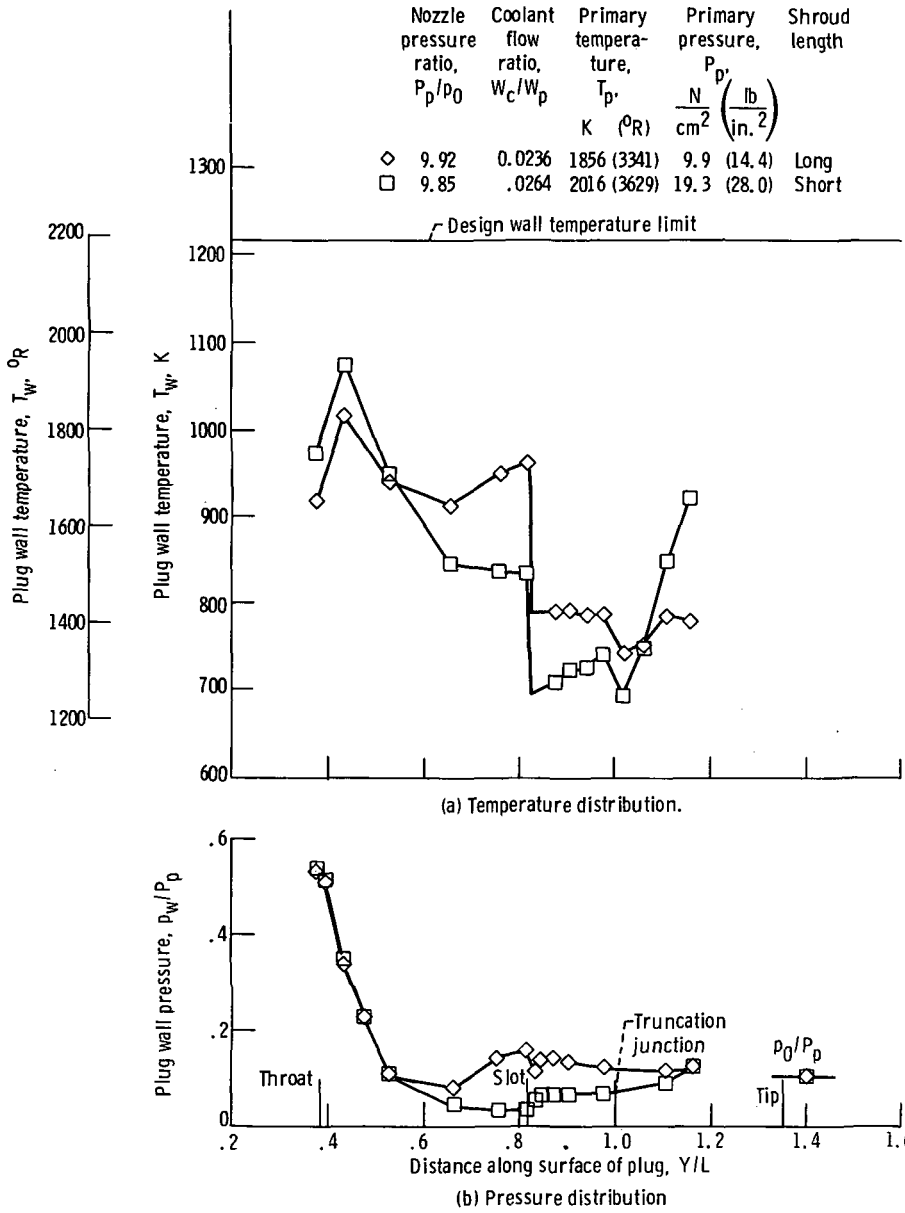

Figure 12. - Effect of shroud length on plug wall temperature and pressure distributions for nozzle pressure ratio $P_p/p_0 = 10$.

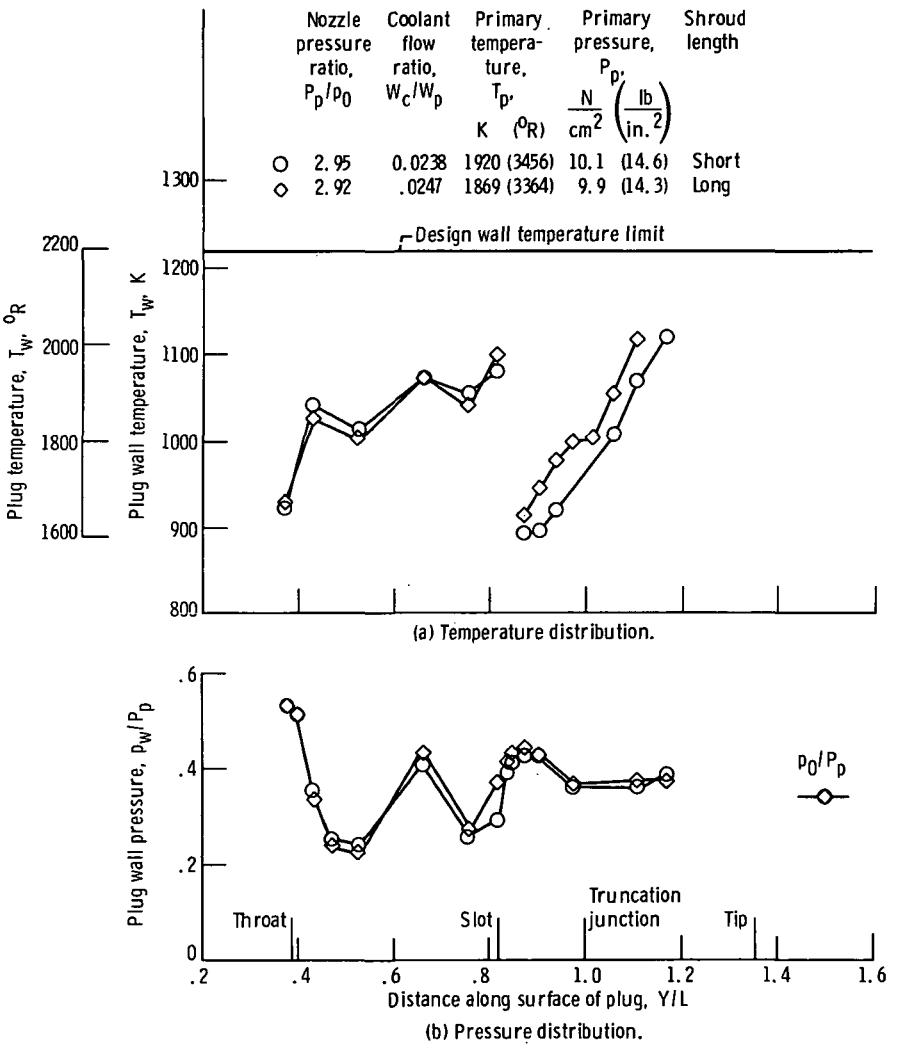

Figure 13. - Effect of outer shroud length on plug wall temperature and pressure distributions for nozzle pressure ratio $P_p/p_0 = 3$.

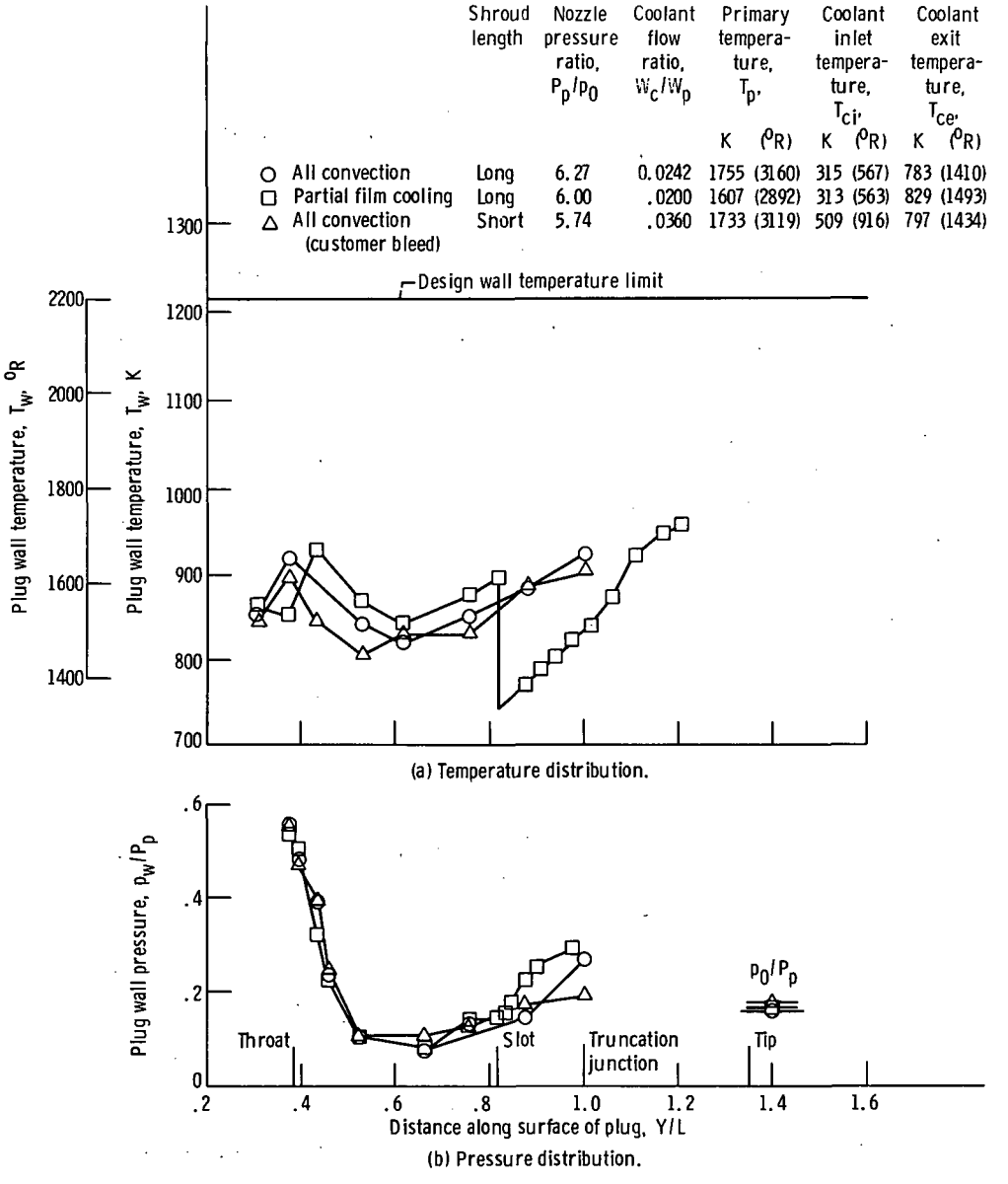

Figure 14. - Comparison of temperature and pressure distributions on partially film cooled with all convective cooled truncated plug.

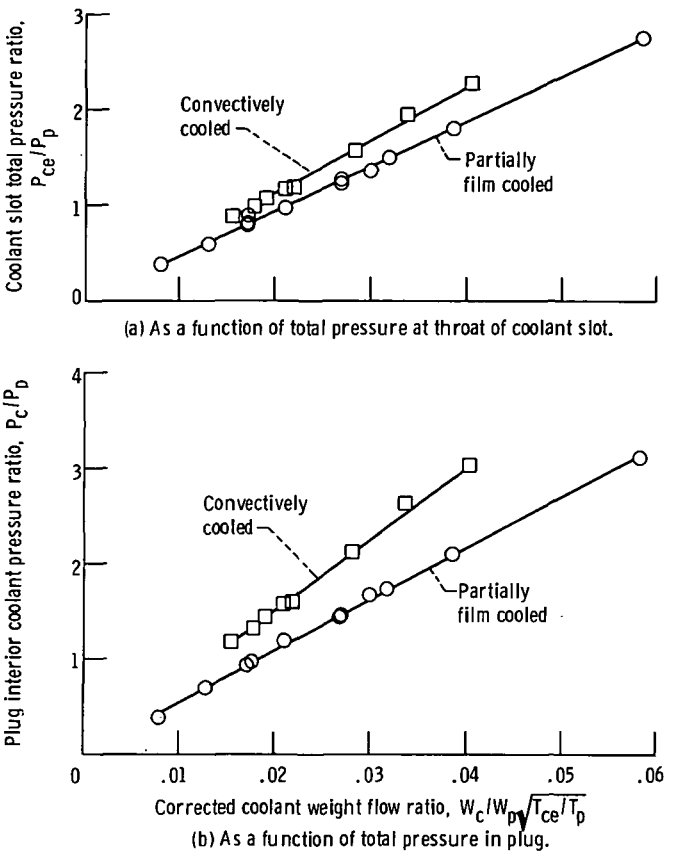

Figure 15. - Comparison of coolant pumping characteristics between partially film cooled plug design and all convectively cooled design.